Electronic Supplementary Material (ESI) for Biomaterials Science.

Supporting Information

A novel donor-acceptor structured diketopyrrolopyrrole-based conjugated polymer synthesized via direct arylation polycondensation (DArP) for highly efficient antimicrobial photothermal therapy

Zhihui Wu,[a] Jing Wang,[a] Linlin Zhao,*[a] Chenxi Li[b] and Yan Lu*[a]

[a] School of Materials Science & Engineering, Tianjin Key Laboratory for Photoelectric Materials and Devices, Key Laboratory of Display Materials &Photoelectric Devices, Ministry of Education, Tianjin University of Technology, Tianjin 300384, China

[b] Key Laboratory of Functional Polymer Materials, College of Chemistry, Nankai University, Tianjin 300071, China

Corresponding authors. E-mail: linlinzhao@email.tjut.edu.cn (L. Zhao); luyan@tjut.edu.cn (Y. Lu)

1. Experimental section

1.1 Materials

2,5-Bis(2-hexyldecyl)-3,6-di(thiophen-2-yl)pyrrolo[3,4-*c*]pyrrole-1,4(2*H*, 5*H*)-dione was bought from SunaTech Inc (Suzhou, China). 2,3-Diethylthieno[3,4-*b*]pyrazine, *N*-bromosuccinimide (NBS) and Herrmann's catalyst were provided by Tianjin heowns Biochemical Technology Co., Ltd. (Tianjin, China). Cesium carbonate (Cs_2CO_3) and tris(o-methoxyphenyl) phosphine (P(*o*-OMePh)$_3$) were purchased from J&K Chemical Ltd. (Beijing, China). DSPE-$MPEG_{2000}$ were purchased from Aivituo Pharmaceutical Technology Co., Ltd. (shanghai, China). 3-(4, 5-dimethyl-2-thiazolyl)-2,5-diphenyl-2-*H*-tetrazolium bromide (MTT) was purchased from Sigma-Aldrich (St. Louis, MO, USA). DMEM, fetal bovine serum (FBS), penicillin, and streptomycin were provided by GibcoBRL (Invitrogen Corp., CA, USA). *Staphylococcus aureus* (*S. aureus*) and *Escherichia coli* (*E. coli*) were obtained from BeNa Culture Collection (Henan, China). Milli-Q water (18.2 MΩ cm^{-2} at 25°C) used throughout the study was purified by using a Millipore filtration system. Other solvents and reagents (analytical grade and spectroscopic grade) were obtained commercially and used as received unless indicated otherwise.

1.2 Instruments

The ^{1}H NMR spectra were recorded on a Bruker AV400 Spectrometer using tetramethylsilane (TMS) as an internal standard for NMR analyses. The gel permeation chromatography (GPC) was measured on a Waters 1525 liquid chromatography system equipped with a Waters 2414 photodiode detector and Waters Styragel HTgel columns using THF as mobile phase at a flow rate of 1.0 mL/min at 35 °C and a series of standard monodisperse polystyrenes were utilized to get a molecular weight calibration curve. UV-vis spectra were carried out on a JASCO V-570. Dynamic light scattering (DLS) measurements were performed using a Zetasizer Nano ZS90c (Malvern Instruments Co., UK) equipped with a He–Ne laser. Cyclic voltammetry (CV) experiments were performed with a LK2005A electrochemical apparatus under a nitrogen atmosphere in a three-necked flask composed of a three-electrodes configuration. All CV measurements were carried out

at room temperature with a conventional three-electrode configuration employing a glassy carbon electrode as the working electrode, a saturated calomel electrode (SCE) as the reference electrode, and a Pt wire as the counter electrode. Dichloromethane was distilled from calcium hydride under dry nitrogen immediately prior to use. Tetrabutylammonium phosphorus hexafluoride (Bu_4NPF_6, 0.1 M) in dichloromethane was used as the supporting electrolyte, and the scan rate was 100 mV s^{-1}. The optimized geometries and HOMO/LUMO levels of the model tetramers of the polymer were obtained by using DFT calculations based on a B3LYP/6-31G* method. Infrared thermal images and temperature changes were recorded using a thermal imaging camera (TiS65, Fluke, Everett, WA, USA). The NIR laser (880 nm) was purchased from Beijing Laserwave Optoelectronics Technology Co., Ltd. (LWIRL880-20W-F, Laserwave, Beijing, China). A FEI Tecnai G2 Spirit TWIN transmission electron microscope (Hillsboro, USA) was used to obtain the transmission electron microscopy (TEM) images of the synthesized nanoparticles. The surface morphologies of bacteria were observed with field emission scanning electron microscopy (SEM) FEI Quanta FEG 250 (FEI, USA).

1.3 Synthesis of DPP2Br

To a solution of 2,5-bis(2-hexyldecyl)-3,6-di(thiophen-2-yl)-2,5-dihydropyrrolo[3,4-*c*]pyrrole-1,4-dione (539.44 mg, 0.72 mmol) in 40 mL of chloroform was added NBS (281.92 mg, 1.58 mmol). The mixture was then stirred in the dark for 17 hours at room temperature. The deionized water (200 mL) was added into the reaction mixture, followed by extraction with chloroform (3 × 50 mL). The organic layers were collected and dried over anhydrous Na_2SO_4. After removal of solvent, the crude product was purified by column chromatography using petroleum ether and dichloromethane (3:1, v/v) as eluent to afford DPP2Br (556.2 mg, 85.2%) as pink solid. ^{1}H NMR (400 MHz, $CDCl_3$) δ 8.62 (d, J = 4.1 Hz, 2H), 7.22 (d, J = 4.2 Hz, 2H), 3.92 (d, J = 7.7 Hz, 4H), 1.87 (q, J = 6.3 Hz, 2H), 1.39 – 1.09 (m, 54H), 0.85 (q, J = 6.5 Hz, 14H).

1.4 Preparation of PDPP-TP nanoparticles (PDPP-TP NPs)

The preparation of PDPP-TP based nanoparticles (PDPP-TP NPs) follows a similar process to PTNPs. Briefly, 2 mg of PDPP-TP was dissolved in 2 mL of tetrahydrofuran (THF), followed by an ultrasonic treatment for 30 min. The homogeneous solution obtained was slowly added into ultrapure water (10 mL). After an ultrasonic treatment for 30 min., the THF was removed by bubbling nitrogen into the solution for 1 h. The resultant solution was transferred to a 50-mL volumetric flask, diluted with deionized water to volume to obtain the stock solution of PDPP-TP NPs with a concentration of 200 μg/mL. The stock solution was stored in refrigerator at 4 °C for later use.

1.5 Determination of loading efficiency and entrapment efficiency

The loading efficiency of the photo-responsive polymer PDPP-TP in the composite nanoparticles (PTNPs) was measured by a spectrophotometric method.[1,2] Briefly, accurately weighed PTNPs (2 mg) was put into 1 mL of THF and incubated in an incubator shaker for 30 min. The absorbance of solution at 903 nm was then measured on a JASCO V-570 UV-vis absorption spectrometer. The amount of PDPP-TP encapsulated in PTNPs was determined on basis of the calibration curve (Fig. 2d). Loading efficiency and entrapment efficiency were calculated by Eqs. (1) and (2), respectively.

$$\text{Loading efficiency (\%)} = \frac{Mass\ of\ PDPP-TP\ in\ PTNPs}{Mass\ of\ PTNPs} \times 100\% \quad (1)$$

$$\text{Entrapment efficiency (\%)} = \frac{Mass\ of\ PDPP-TP\ in\ PTNPs}{Mass\ of\ PDPP-TP\ in\ feed} \times 100\% \quad (2)$$

1.6 Photothermal property

PTNPs aqueous dispersions with different concentrations (10, 20, 30, 70, 100 μg/mL) were irradiated with 880 nm laser at a power density of 0.7 W/cm^2 for 15 min to evaluate the effect of PTNPs concentration on their photothermal performance. Similarly, PTNPs aqueous dispersions at 30 μg/mL were also irradiated with 880 nm laser at different power densities (0.3, 0.5, 0.7, 1.0,

1.2 W/cm^2) for 15 min to inspect the effect of laser power density on the photothermal performance of PTNPs. In this study, the temperature was recorded at intervals of 30 seconds with a thermal imaging camera (TiS65, Fluke, Everett, WA, USA).

1.7 Photothermal conversion efficiency (PTCE)

The photothermal conversion efficiency of PTNPs was calculated from the lifting and cooling curves.[3-5] PTNPs aqueous dispersions (30 μg/mL) were irradiated by 880 nm laser at 0.7 W/cm^2 for 10 min, and then the solution was cooled down naturally to ambient temperature. The temperature of the solution was recorded at intervals of 30 s during this process. The photothermal conversion efficiencies (η) can be calculated according to the standard method as described in our recent work.[4,5]

1.8 Photostability

The samples of PTNPs (30 μg/mL) and the reference ICG (30 μg/mL) were separately irradiated with 880 nm laser (0.7 W/cm^2) for 10 min. The laser was then turned off and the sample was cooled to the room temperature naturally. The temperature of samples was recorded using the IR thermal camera every 30 s. Subsequently, the cycle of heat-up and cooling were repeated four times.

1.9 Dark toxicity and in vitro phototoxicity

The dark cytotoxicity and in vitro phototoxicity of PTNPs were evaluated using the MTT assay.[4-6] To assess the dark toxicity of PTNPs, HeLa cells (1×10^4 cells/well) were seeded onto 96-well plates in 200 μL of DMEM and allowed to attach for 24 h. After cell attachment, the medium was replaced with 100 μL of fresh medium containing PTNPs with a series of concentration (0, 10, 20, 30, 60, 90, and 120 μg/mL), and then incubated for 24 h. The cell viability was assessed by MTT assay. Three independent experiments were performed to obtain error bars. In vitro phototoxicity of PTNPs was also studied according to the above similar procedure, except that

PTNPs-loaded HeLa cells were irradiated with an 880 nm laser at 0.7 W/cm^2 for 5 min prior to 24 h incubation.

Table S1. Comparison the photothermal antibacterial performance of NIR light triggered conjugated polymer-based photoactive materials.

Photoactive material	Modality	PTCE	Irradiation conditions	Bacteria	Antibacterial efficiency	Ref.
DMCPNs	PTT and PDT	69%	808 nm (550 mW/cm^2, 5 min) and white light (65 mW/cm^2, 5 min)	Amp^r *E. coli*	98%	[7]
CPNs-TAT/ PMNT	PTT and PDT	57.48%	808 nm (0.7 W/cm^2, 5 min) and white light (30 mW/cm^2, 10 min)	*E. coli*	99%	[8]
				S. aureus	99%	
				A. niger	70%	
PTDBD	PTT and PDT	31%	808 nm (1.0 W/cm^2, 8 min)	*E. coli*	99.3%	[9]
				S. aureus	98.9%	
				C. albicans	90%	
PEDOT:ICG@PEG-GTA	PTT and PDT	71.1%	1064 nm (1.5 W/cm^2，5 min) and 808 nm (1.5 W/cm^2，5 min)	*E. coli*	~99%	[10]
				S. aureus	~99%	
WMG1	PTT	60%	808 nm (0.75 W/cm^2, 6 min)	*E. coli*	96%	[11]
				B. subtilis	-	
CPNs-Tat	PTT	34%	808 nm (2 W/cm^2, 5 min)	*E. coli*	~99.8%	[12]
				S. aureus	~90%	
				C. albicans	~100%	
BTB/PTDBD/CS	PTT	31%	808 nm (1.0 W/cm^2, 8 min)	*E. coli*	-	[13]
				K. pneumoniae		
				S. aureus		
PDTPBT	PTT	71.1%	808 nm (1.0 W/cm^2, 6 min)	*E. coli*	92.8%	[14]
				MRSA	92.2%	

P1	PTT	33±1%	808 nm (0.75 W/cm^2, 6 min)	*E. coli*	~100%	[15]
				B. subtilis	~99%	
pPCP-NPs	PTT	51.5%	1064 nm (1.0 W/cm^2, 10 min)	*E. coli*	~100%	[16]
				S. aureus	~100%	
SP-PPh_3 NPs	PTT	43.8%	808 nm (1.0 W/cm^2, 6 min)	*E. coli*	99.4%	[17]
				S. aureus	98.6%	
PTNPs	PTT	52.8%	880 nm (0.7 W/cm^2, 6 min)	*E. coli*	100%	This work
				S. aureus	100%	

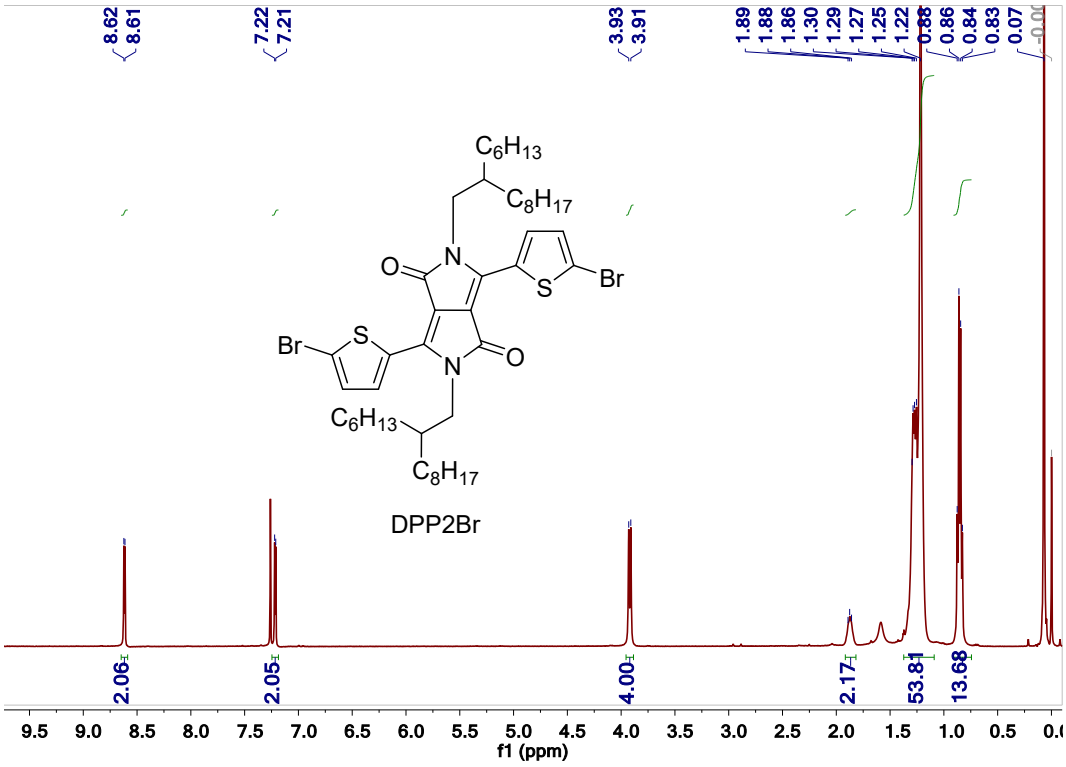

Fig. S1 ^{1}H NMR spectrum of DPP2Br in $CDCl_3$.

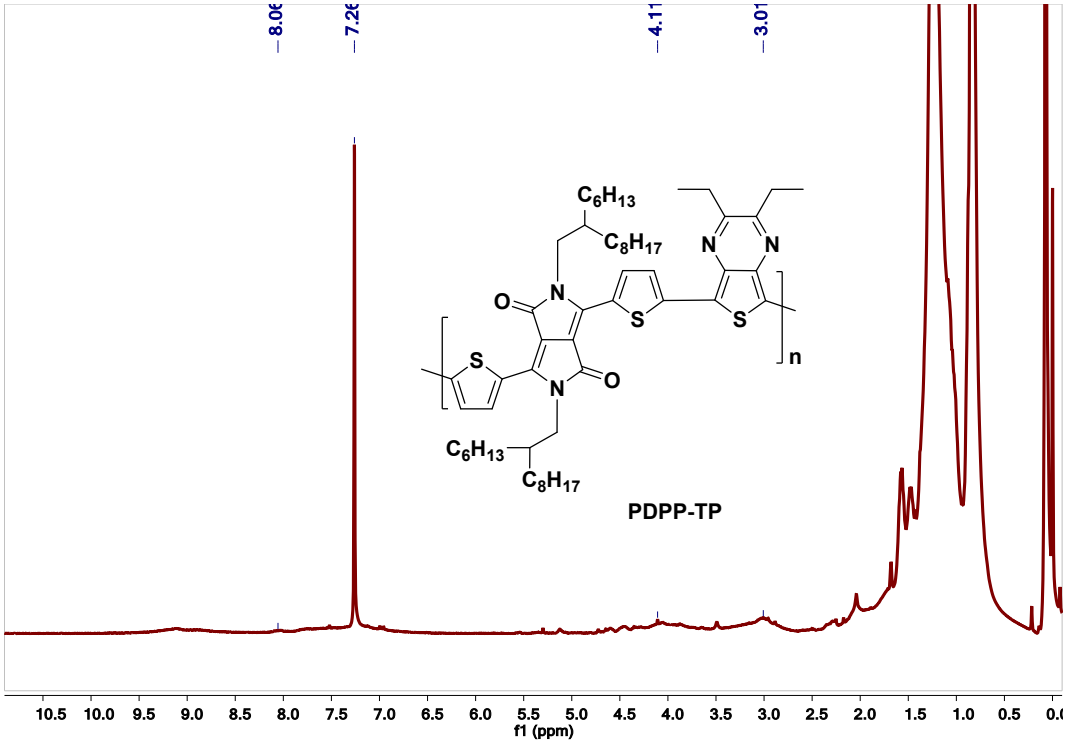

Fig. S2 ^{1}H NMR spectrum of PDPP-TP in $CDCl_3$.

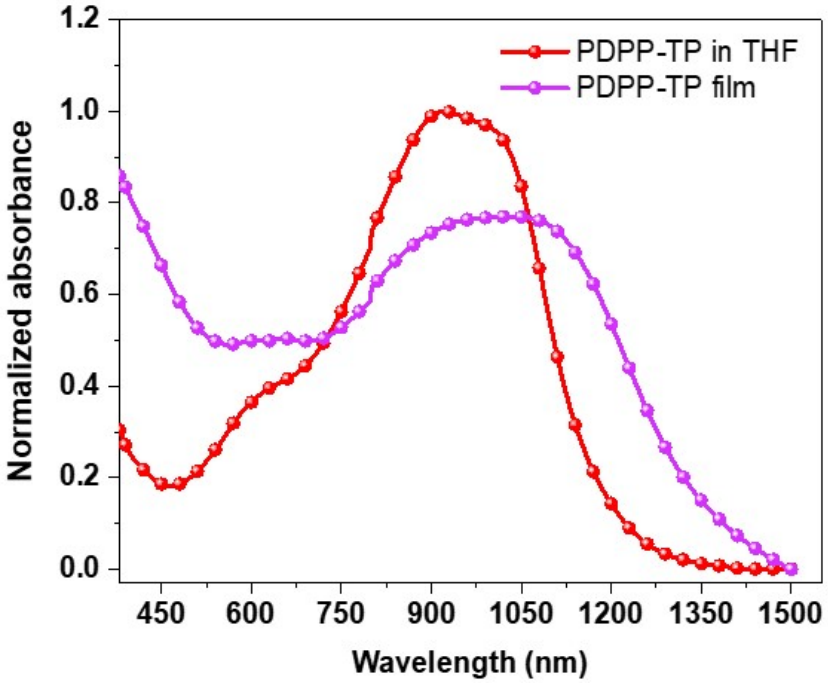

Fig. S3 Normalized absorption spectra of PDPP-TP in THF (30 μg/mL) and PDPP-TP film (spin-cast from THF solution).

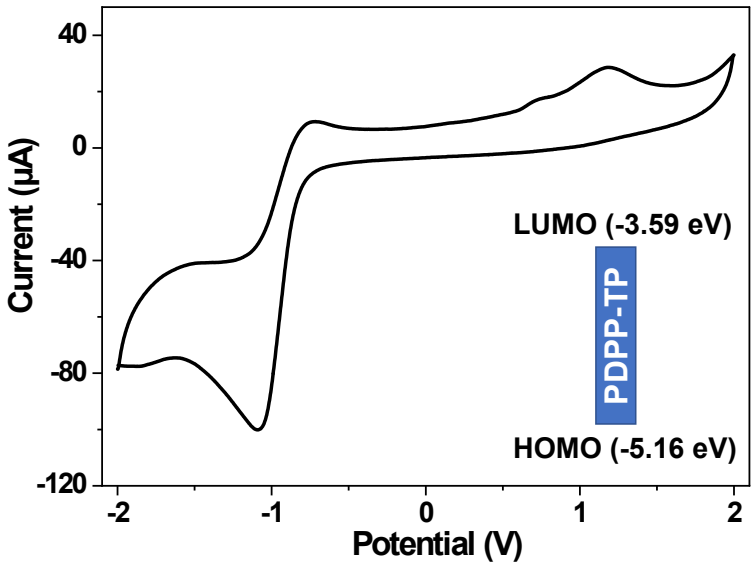

Fig. S4 CV curve and energy levels diagram.

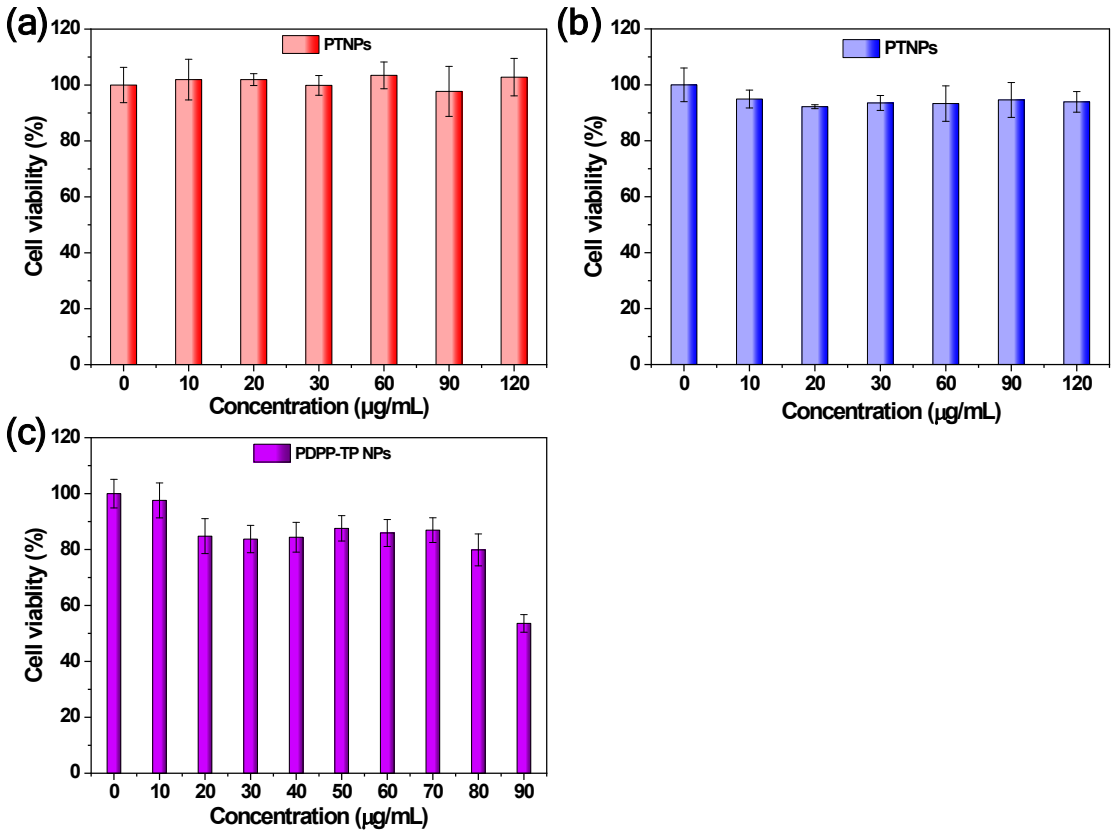

Fig. S5 Effect of PTNPs and PDPP-TP NPs concentrations on cell viability. HeLa cells (a, c) and L929 (b).

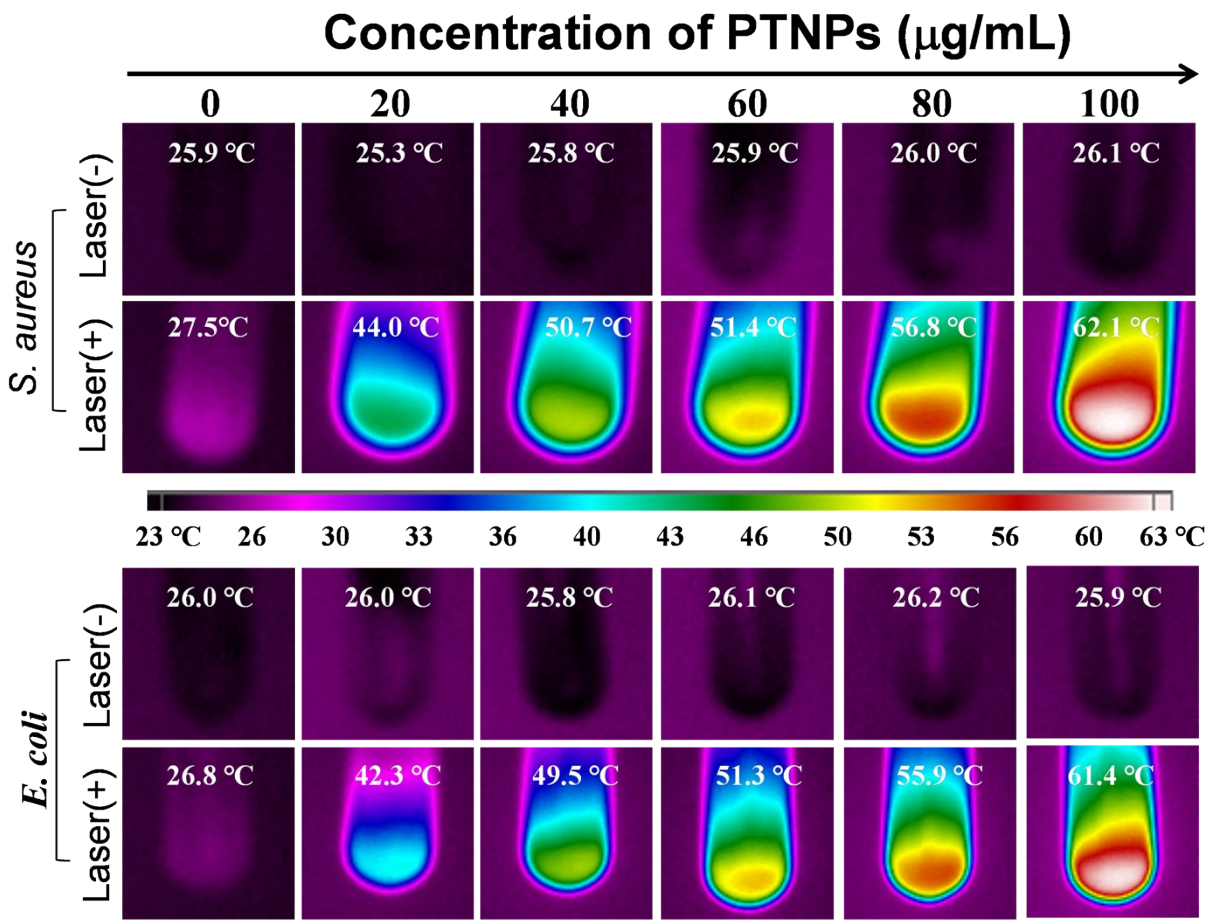

Fig. S6 Thermal images recorded for *S. aureus* and *E. coli* treated with PTNPs at different concentrations in the dark (Laser(-) group) and under 880 nm laser irradiation at 0.7 W/cm^2 for 6 min (Laser(+) group).

References

1. Y. B. Xu, Y. X. Zi, J. F. Lei, X. Y. Mo, Z. L. Shao, Y. Y. Wu, Y. Tian, D. F. Li and C. D. Mu, *Carbohydr. Polym.,* 2020, **233**, 115858.
2. C. Sahub, G. Tumcharern, P. Chirawatkul, V. Ruangpornvisuti, S. Ekgasit, S. Wanichweacharungruang, T. Tuntulani, T. Palaga and B. Tomapatanaget, *Colloids Surf. B.*, 2017, **156**, 254–261.
3. X. Z. Li, L. Liu, S. L. Li, Y. P. Wan, J. X. Chen, S. Tian, Z. M. Huang, Y. F. Xiao, X. Cui, C. Y. Xiang, Q. L. Tan, X. H. Zhang, W. S. Guo, X. J. Liang and C. S. Lee, *ACS Nano*, 2019,

13, 12901−12911.

4. Z. He, L. L. Zhao, Q. Zhang, M. J. Chang, C. X. Li, H. S. Zhang, Y. Lu and Y. S. Chen, *Adv. Funct. Mater*., 2020, **30**, 1910301.
5. W. Y. Jia, F. F. Huang, Q. Zhang, L. L. Zhao, C. X. Li and Y. Lu, *Chem. Commun*., 2022, **58**, 6340-6343.
6. T. T. Sun, X. X. Chen, X. Wang, S. Liu, J. Liu and Z. G. Xie, *Mater. Chem. Front*., 2019, **3**, 127-136.
7. H. J. Zhang, Y. C. Liang, H Zhao, R. L. Qi, Z Chen, H. X. Yuan, H. Y. Liang and L. Wang, *Macromol. Biosci.*, 2020, **20**, 1900301.
8. Q. F. Cui, H. B. Yuan, X. Y. Bao, G. Ma, M. M. Wu and C. F. Xing. *ACS Appl. Bio Mater*., 2020, **3**, 4436-4443.
9. S. Y. Zhou, Z. J. Wang, Y. X. Wang and L. H. Feng, *ACS Appl. Bio Mater*., 2020, **3**, 1730-1737.
10. L. Y. Li, Y. X. Liu, P. L. Hao, Z. G. Wang, L. M. Fu, Z. F. Ma and J. Zhou, *Biomaterials*, 2015, **41**, 132-140.
11. B. Wang, G. X. Feng, M. Seifrid, M. Wang, B. Liu and G. C. Bazan, *Angew. Chem. Int. Ed.*, 2017, **56**, 16063–16066.
12. Y. X. Wang, S. L. Li, L. B. Liu and L. H. Feng, *ACS Appl. Bio Mater.*, 2018, **1**, 27-32.
13. H. P. Wang, S. R. Zhou, L. X. Guo, Y. X. Wang and L. H. Feng, *ACS Appl. Mater. Interfaces*, 2020, **12**, 39685-39694.
14. C. Zhang, K. G. Wang, X. Y. Guo and Y. L. Tang, *J. Mater. Chem. C*, 2022, **10**, 2600-2607.
15. G. X. Feng, C. K. Mai, R. Y. Zhan, G. C. Bazan and B. Liu, *J. Mater. Chem. B*, 2015, **3**, 7340-7346.
16. H. L. Zhou, D. S. Tang, X. X. Kang, H. T. Yuan, Y. J. Yu, X. L. Xiong, N. E. Wu, F. Z. Chen, X. Wang, H. H. Xiao and D. S. Zhou, *Adv. Sci*., 2022, **9**, 2200732.
17. G. Y. Pan, Y. W. Li, L. J. Ma, Y. F. Ma, W. T. Ai, Z. G. Wang, X. H. Hou, V. Z. Grigory and Z. Wang, *Chem. J. Chin. Univ.*, 2020, **41**, 670-681.